Published in final edited form as:
Nature. ; 474(7352): 521–525. doi:10.1038/nature10136.

Agonist-bound adenosine A_{2A} receptor structures reveal common features of GPCR activation

Guillaume Lebon, **Tony Warne**, **Patricia C. Edwards**, **Kirstie Bennett**[1], **Christopher J. Langmead**[1], **Andrew G.W. Leslie**, and **Christopher G. Tate**[*]
MRC Laboratory of Molecular Biology, Hills Road, Cambridge CB2 0QH, UK

[1]Heptares Therapeutics, BioPark, Broadwater Road, Welwyn Garden City AL7 3AX, UK

The adenosine receptors and β-adrenoceptors (βARs) are G protein-coupled receptors (GPCRs) that activate intracellular G proteins upon binding agonist such as adenosine[1] or noradrenaline[2], respectively. GPCRs have similar structures consisting of 7 transmembrane helices that contain well-conserved sequence motifs, suggesting that they are probably activated by a common mechanism[3,4]. Recent structures of βARs highlight residues in transmembrane region 5 that initially bind specifically to agonists rather than to antagonists, suggesting an important role in agonist-induced activation of receptors[5-7]. Here we present two crystal structures of the thermostabilised human adenosine A_{2A} receptor (A_{2A}R-GL31) bound to its endogenous agonist adenosine and the synthetic agonist NECA. The structures represent an intermediate conformation between the inactive and active states, because they share all the features of GPCRs that are thought to be in a fully activated state, except that the cytoplasmic end of transmembrane helix 6 partially occludes the G protein binding site. The adenine substituent of the agonists bind in a similar fashion to the chemically-related region of the inverse agonist ZM241385[8]. Both agonists contain a ribose group, not found in ZM241385, which extends deep into the ligand binding pocket where it makes polar interactions with conserved residues in H7 (Ser277$^{7.42}$ and His278$^{7.43}$; superscripts refer to Ballesteros-Weinstein numbering[9]) and non-polar interactions with residues in H3. In contrast, the inverse agonist ZM241385 does not interact with any of these residues and comparison with the agonist-bound structures suggests that ZM241385 sterically prevents the conformational change in H5 and therefore it acts as an inverse agonist. Comparison of the agonist-bound structures of A_{2A}R with the agonist-bound structures of β-adrenoceptors suggests that the contraction of the ligand binding pocket caused by the inward motion of helices 3, 5 and 7 may be a common feature in the activation of all GPCRs.

In the simplest model for the conformational dynamics of GPCRs[10] there is an equilibrium between two states, R and R*. The inactive state R preferentially binds inverse agonists and the activated state R* preferentially binds agonists[11]. Only R* can couple and activate G proteins. Although there are far more complex schemes[12] describing intermediates between R and R*, studies on rhodopsin have indicated that there is only one major conformational change that significantly alters the structure of the receptor[3]. Thus the structures of dark-

[*]Corresponding author: MRC Laboratory of Molecular Biology, Hills Road, Cambridge CB2 0QH, UK, cgt@mrc-lmb.cam.ac.uk, Telephone +44-(0)1223-402266, Fax +44-(0)1223-213556 .
Author contributions. G.L. devised and performed receptor expression, purification, crystallization, cryo-cooling of the crystals, data collection, data processing and structure refinement. T.W. and P.C.E. helped with expression, crystal cryo-cooling and data collection. K.B. performed the radioligand binding assays and pharmacological analyses on receptor mutants in whole cells and C.L. was involved in data analysis and experimental design. A.G.W.L. was involved in data processing and structure refinement. Manuscript preparation was performed by G.L., A.G.W.L. and C.G.T. The overall project management was by C.G.T.
Author Information. Co-ordinates and structure factors have been submitted to the PDB database under accession codes 2YDO and 2YDV for A_{2A}R-GL31 bound either to adenosine or NECA, respectively.

Europe PMC Funders Author Manuscripts

state rhodopsin[13,14] and of opsin[15,16] are considered to be representative structures for the R and R* state, respectively. Structures of 6 different GPCRs[8,13,17-21] in conformations closely approximating to the R state have now been determined and it is clear that they are similar to each other, with RMSDs between any pair of structures in the transmembrane domains being less than 3 Å. As observed in light-activation of rhodopsin, the major structural difference between R and R* is the movement of the cytoplasmic ends of helices 5 and 6 away from the receptor core by 5-6 Å, opening up a cleft in the centre of the helix bundle where the C-terminus of a G protein can bind[16]. Recently, the structure of an agonist-bound β-adrenoceptor (β_2AR) was determined in complex with an antibody fragment (nanobody Nb80)[5]. This structure of β_2AR is very similar to the structure of opsin, which suggests that the nanobody mimicked the action of a G protein by maintaining the receptor structure in an activated state. Given the structural similarities between opsin and the β_2AR-Nb80 complex, it is likely that the structures of the R* states of other GPCRs are also highly similar. This is consistent with the same heterotrimeric G proteins being able to couple to multiple different receptors[22]. However, do the conserved structures of R and R* imply that all agonists activate the receptors in an identical fashion? The recent structures of a thermostabilised β_1AR bound to 4 different agonists suggested that a defining feature of agonist binding to this receptor is the formation of a hydrogen bond with Ser$^{5.46}$ on transmembrane helix 5 that accompanies the contraction of the ligand binding pocket[7]. Here we describe two structures of the adenosine A_{2A} receptor (A_{2A}R) bound to two different agonists, which suggests that the initial action of agonist binding to A_{2A}R has both similarities and differences compared to agonist binding in βARs.

The native human A_{2A}R when bound to its endogenous agonist adenosine or to the high-affinity synthetic agonist NECA is unstable in detergent, so crystallization and structure determination relied on using a thermostabilised construct (A_{2A}R-GL31) that contained four point mutations, which dramatically improved its thermostability. Pharmacological analysis showed that the mutant receptor bound the five antagonists tested with greatly reduced affinity (1.8 - 4.3 log units), whereas four agonists bound with similar affinity to the wild-type receptor (Supplementary Fig. 1). However, A_{2A}R-GL31 is only weakly activated by the agonist CGS21680 (Supplementary Fig. 2), which suggests that the thermostabilising mutations might also decouple high-affinity agonist binding from the formation of R*. The conformation of GL31 is not consistent with it being in the fully-activated G protein coupled state, because we do not observe a 42-fold increase in affinity for NECA binding measured for $G_{\alpha s}$-coupled A_{2A}R[23]. These data all suggest that A_{2A}R-GL31 is in an intermediate conformation between R and R*, which is consistent with the structural analysis presented below.

The two structures we have determined are of A_{2A}R-GL31 bound to adenosine and NECA with resolutions of 3.0 Å and 2.6 Å, respectively (Supplementary Table 1). Global alignments of the A_{2A}R-GL31 structures with A_{2A}-T4L (A_{2A}R with T4 lysozyme inserted into inner loop 3) bound to the inverse agonist ZM241385 were performed based on those residues in the region of the ligand binding pocket that show the closest structural homology (Fig. 1 and Supplementary Text). This gave an rmsd in Cα positions of 0.66 Å for the 96 atoms selected, which include all residues involved in binding either adenosine or NECA, with the exception of those in H3. Using this transformation, the adenine-like moiety of the two ligands superimposes almost exactly (rmsd 0.56 Å). The most significant differences between the two structures are seen in a distortion and a 2 Å shift primarily along the helical axis of H3, a bulge in H5 (resulting from non-helical backbone conformation angles of residues Cys185 and Val186) that shifts residues into the binding pocket by up to 2 Å and also a change in conformation of the cytoplasmic ends of H5, H6 and H7 (Fig. 1). Comparison of the A_{2A}R-GL31 structure with the agonist-bound β_2AR-Nb80 complex indicates that these differences are similar to the conformational changes in the β_2AR that

are proposed to be responsible for the formation of the R* state[5]. However, it is unlikely that the structure of A_{2A}R-GL31 represents the fully activated state, because comparison with opsin bound to the C-terminal peptide of the G protein transducin shows that there is insufficient space in A_{2A}R-GL31 for the C-terminus of the G protein to bind (Supplementary Fig. 3). This is based on the assumption that all G proteins bind and activate GPCRs in a similar fashion, but given the highly-conserved structures of both G proteins and GPCRs this seems a reasonable hypothesis.

The fact that the structure of A_{2A}R-GL31 represents an agonist-binding state is consistent with how A_{2A}R-GL31 was engineered. Thermostabilising mutations were selected by heating the NECA-bound detergent-solubilised receptor, so the mutations are anticipated to stabilize the agonist-bound state either by stabilizing helix-helix interactions and/or biasing the conformational equilibrium between the agonist-bound R* state and the agonist bound R-state[24-26]. The two most thermostabilising mutations, L48A and Q89A, are in regions of the receptor that are involved in transitions between R and R*, providing a possible explanation for their thermostabilising effect (Supplementary Fig. 4). The other two mutations, A54L and T65A, are at the receptor-lipid interface and the reason for their thermostabilising effect is unclear. Although the overall shape of the ligand binding pockets of A_{2A}R and β_2AR are different, the structural similarities with the β_2AR-Nb80[5] and the structural differences to ZM241385-bound A_{2A}-T4L[8] indicate that the structure of the binding pocket in A_{2A}R-GL31 is a good representation of the agonist-bound binding pocket of the wild-type receptor (Fig.1).

Adenosine and NECA bind to A_{2A}R-GL31 in a virtually identical fashion, in addition, the adenine ring in the agonists interacts with A_{2A}R in a similar way to the chemically-related triazolotriazine ring of the inverse agonist ZM241385 (Fig. 2). Thus the hydrogen bonds between exocyclic adenosine N6 (Supplementary Fig. 5) with both Glu169 in extracellular loop 2 (EL2) and Asn253$^{6.55}$ in H6 are similar, with the significant π-stacking interaction with Phe168 in EL2 also conserved. One of the major structural differences between ZM241385 and the agonists is the presence of a furan substituent on C20 of triazolotriazine in the inverse agonist, whilst agonists contain a ribose substituent linked to N9 of adenine (Fig. 2 and Supplementary Fig. 5). In ZM241385, the furan group forms a hydrogen bond with Asn253$^{6.55}$ in H6 and van der Waals contacts with other residues in H3, H5 and H6[8]. In contrast, the ribose moiety in agonists forms hydrogen bonds with Ser277$^{7.42}$ and His278$^{7.43}$ in H7, in addition to van der Waals interactions with other residues in H3 and H6 (Fig. 2). In particular, Val84$^{3.32}$ has to shift its position upon agonist binding due to a steric clash with the ribose ring, which may contribute to the 2 Å shift observed in H3 (Fig. 3). These differences in binding between ZM241385 and either adenosine or NECA suggest that the residues that bind uniquely to agonists (Ser277$^{7.42}$ and His278$^{7.43}$) play a key role in the activation of the receptor, as previously shown by mutagenesis studies[27,28]. This is analogous to the situation in the activation of β_1AR, where only full agonists cause the rotamer conformation changes of Ser$^{5.46}$ in H5, whereas the inverse agonist ICI118551 prevents receptor activation by sterically blocking the rotamer change[7,29]. However, the details of the activation differ in that the critical residues that bind agonists and not antagonists are in H5 in β_1AR, but in H7 in A_{2A}R (Fig. 4).

Adenosine and NECA activate the A_{2A}R through interactions with H3 and H7 that are absent in the interactions between the receptor and the inverse agonist ZM241385 (Fig. 2). The inward shift of H7, the movement of H3 and the consequent formation of a bulge in H5 are all observed in the structure of agonist-bound A_{2A}R-GL31 and β_2AR-Nb80 (Fig.1). The formation of the bulge in H5 of the β_2AR-Nb80 structure was linked to a series of conformational changes that generates the 60° rotation of H6 about Phe282$^{6.44}$, resulting in the cytoplasmic end of H6 moving out from the receptor centre and opening the cleft where

the C terminus of a G protein is predicted to bind as observed in opsin[5,6]. There are analogous side chain movements in A_{2A}R-GL31 that result in a 40° rotation of H6, but the cytoplasmic end of H6 remains partially occluding the G protein-binding cleft (Supplementary Fig. 3), perhaps because the fully active conformation requires the binding of G proteins to stabilize it. Interestingly, the structure of β_2AR[6] with a covalently bound agonist is also not in the fully activated R* conformation, which is only seen after the nanobody Nb80 is bound[5]. The importance of the bulge in H5 in the activation of A_{2A}R is highlighted by how inverse agonists bind. Formation of the H5 bulge results in the inward movement of Cys185$^{5.46}$ (Cβ moves by 4 Å), which in turn causes the movement of Val186 and ultimately a shift of His250$^{6.52}$ by 2 Å into the ligand binding pocket thereby sterically blocking the binding of ZM241385 (Supplementary Fig. 4). Hence, when the inverse agonist binds, it is anticipated that the H5 bulge is unlikely to form due to the opposite series of events and hence the formation of the R* state is inhibited.

Thus in both βARs and A_{2A}R, the formation of the H5 bulge seems to be a common action of agonists, whereas inverse agonists seem to prevent its formation. However, the energetic contributions to its formation may be different between the two receptors. In the βARs there is a major contribution from direct interaction between the agonist and Ser$^{5.46}$, while in the A_{2A}R, the major interaction appears to come from polar interactions involving residues in H7 combined with interactions between the agonist and H3. Despite these differences, agonist binding to both receptors involves strong attractive non-covalent interactions that pull the extracellular ends of H3, H5 and H7 together, which is the necessary prerequisite to receptor activation.

While this manuscript was in review, a related manuscript appeared[30], describing the structure of the A_{2A}-T4L chimera bound to the agonist UK432097, which is identical to NECA except for two large substituents on the adenine ring. The structure of UK432097-bound A_{2A}-T4L is very similar to the structures presented here in the transmembrane regions (rmsd 0.6 Å), although there are differences in the extracellular surface due to the bulky extensions of UK432097 interacting with the extracellular loops and the absence of density for residues 149-157. Xu *et al.* conclude that the structure of UK432097-bound A_{2A}-T4L is in an “active state configuration”, whereas we conclude that the NECA- and adenosine-bound structures are best defined as representing an intermediate state between R and R*.

METHODS SUMMARY

Expression, purification and crystallization

The thermostabilised A_{2A}R-GL31 construct contains amino acid residues 1-316 of the human A_{2A}R, four thermostabilising point mutations (L48A$^{2.46}$, A54L$^{2.52}$, T65A$^{2.63}$ and Q89A$^{3.37}$) and the mutation N154A to remove a potential N-glycosylation site. A_{2A}R-GL31 was expressed in insect cells using the baculovirus expression system and purified in the detergent octylthioglucoside using Ni^{2+}-NTA affinity chromatography and size exclusion chromatography (see Online Methods). The purified receptor was crystallized in the presence of cholesteryl hemisuccinate by vapour diffusion, with the conditions described in Online Methods.

Data collection, structure solution and refinement

Diffraction data were collected in multiple wedges (20° per wedge) from a single cryo-cooled crystal (100 K) for the GL31-NECA complex at beamline ID23-2 at ESRF, Grenoble, France and from 4 crystals for the GL31-adenosine complex, at beamline I24 at Diamond, Harwell, UK. The structures were solved by molecular replacement using the

ZM241385-bound A_{2A}-T4L structure (PDB code 3EML)[8] as a model (see Online Methods). Data collection and refinement statistics are presented in Supplementary Table 1 and omit densities for the ligands are shown in Supplementary Fig. 6.

Supplementary Material

Refer to Web version on PubMed Central for supplementary material.

Acknowledgments

This work was supported by core funding from the MRC, and grants from Heptares Therapeutics Ltd and from BBSRC (BB/G003653/1). We would like to thank F. Magnani for technical help at the start of the project and F. Gorrec for developing the crystallization screen. We also thank the beamline staff at the European Synchrotron Radiation Facility, particularly at (beamline ID23-2; D. Flot and A. Popov), the Swiss Light Source (beamline X06SA; Villigen, Switzerland) and at Diamond (beamline I24; G. Evans, D. Axford and R. Owen). F. Marshall, M. Weir, M. Congreve and R. Henderson are thanked for their helpful comments on the manuscript.

Appendix

METHODS ONLINE

Expression, purification and crystallization

The human A_{2A} construct, GL31, contains four thermostabilising point mutations ($L48A^{2.46}$, $A54L^{2.52}$, $T65A^{2.63}$ and $Q89A^{3.37}$), the mutation N154A to remove the potential N-glycosylation site and a truncation at the C-terminus after Ala316 (Ref [32]). A polyhistidine tag (His_{10}) was engineered at the C-terminus, separated from the receptor by a TEV protease cleavage site. Baculovirus expression and membrane preparation were performed as described previously for the β_1AR[33].

Membranes were thawed at room temperature, diluted with 25 mM Hepes pH 7.4, in presence of protease inhibitors (Complete™, Boehringer). Membranes were pre-incubated with NECA at 100 μM for 45 minutes at room temperature. The receptor-ligand complexes were then solubilised by adding decylmaltoside (DM) and NaCl to give final concentrations of 1.5% and 0.3M, respectively, stirred for 30 minutes (4°C) and insoluble material removed by ultracentrifugation (120,000 *g*, 45 minutes, 4°C). All protein purification steps were performed at 4°C. The solubilised receptor sample was filtered through a 0.22 μm filter (Millipore) and applied to a 5 ml Ni-NTA superflow cartridge (Qiagen) pre-equilibrated with buffer (25 mM Hepes, pH 7.4, 0.1 M NaCl, 100 μM NECA, 0.15% DM, 2.5 mM imidazole). The column was washed sequentially with the same buffer supplemented with either 10, 40 or 80 mM imidazole, and then eluted with 250 mM imidazole. The eluted receptor-ligand complex was mixed with His_6-tagged TEV protease to cleave the tag for 4-6 hours, 4°C, concentrated to 2 ml using an Amicon-ultra spin concentrator (Ultracel-50K, Millipore) and then imidazole was removed using a PD-10 column (GE Healthcare). Eluted fractions were further purified by binding the TEV and other contaminants to Ni-NTA (QIAGEN) pre-equilibrated in 25 mM Hepes pH 7.4, 0.1 M NaCl, 100 μM NECA, 0.15% DM, 40 mM imidazole, incubating for 30 minutes and then collecting the flow-through. For detergent exchange into 0.35% octylthioglucoside (OTG), the sample was concentrated using an Amicon-ultra concentrator (Ultracel-50K, Millipore), diluted 10-fold in 25 mM Hepes pH 7.4, 0.1 M NaCl, 100 μM NECA, 0.35% OTG, and concentrated again to 0.3 ml. The protein sample was applied to a Superdex 200 10/300 GL size exclusion column pre-equilibrated in 25 mM Hepes pH 7.4, 0.1 M NaCl, 100 μM NECA, 0.35% OTG and run at 0.5 ml/minute. Eluted receptor fractions (2-2.5 ml) were concentrated to 50-60 μl. Protein determination was performed using the amido black[34] assay.

Europe PMC Funders Author Manuscripts

Before crystallization, cholesteryl hemisuccinate (CHS) and OTG were added to 1 mg/ml and 0.5% respectively and the protein concentration adjusted to 10-12.5 mg/ml. NECA and adenosine A_{2A}-GL31 crystal hits were obtained using a new PEG-based crystallisation screen developed in house[35]. Crystals were grown at 4°C in 100 nl sitting drops using 0.05 M ADA NaOH, pH 6.4, 23.6% PEG 400, 4% v/v 2-propanol for the NECA complex. Crystals were cryo-protected by soaking in 0.05 M ADA NaOH, pH 6.4, 45% PEG 400. For the adenosine complex, crystals were initially grown in 0.05 M TrisHCl, pH 7.6, 9.6% PEG 200, 22.9%. PEG 300. Crystals were cryo-protected by soaking in 0.05 M TrisHCl, pH 7.5, 15% PEG 200, 30% PEG 300. The crystals were mounted on Hampton CrystalCap HT loops and cryo-cooled in liquid nitrogen.

Data collection, structure solution and refinement

Diffraction data for the NECA complex were collected at the European Synchrotron Radiation Facility, Grenoble with a Mar 225 CCD detector on the microfocus beamline ID23-2 (wavelength, 0.8726 Å) using a 10 μm focused beam and for the adenosine complex on beamline I24 at the Diamond Light Source, Harwell with a Pilatus 6M detector and a 10 μm microfocus beam (wavelength 0.9778 Å). The microfocus beam was essential for the location of the best diffracting parts of single crystals, as well as allowing several wedges to be collected from different positions. Images were processed with MOSFLM[36] and SCALA[37]. The NECA complex was solved by molecular replacement with PHASER[38] using the A_{2A}-T4L structure (PDB code 3EML)[8] as a model after removal of the coordinates for T4L, all solvent molecules and the inverse agonist ZM241384. This structure was then used as a starting model for the structure solution of the adenosine complex. Refinement and rebuilding were carried out with REFMAC5[39] and COOT[40] respectively. In the final models, 98.1% of residues were in the favoured region of the Ramachandran plot with one outlier for the NECA complex, and 97.7% with no outliers for the adenosine complex. Smile strings for NECA and adenosine were created using Sketcher and dictionary entries using Libcheck. Hydrogen bond assignments for the ligands were determined using HBPLUS[41].

To facilitate a structural comparison between ZM241385-bound A_{2A}-T4L and the thermostabilised A_{2A}-GL31 with bound agonist, the structures were superimposed based on those residues in the region of the ligand binding pocket that show the closest structural homology. This was achieved using the lsq_improve option of the program O[42] and an initial transformation based on residues at the C-terminus of helix 6 and the N-terminus of helix 7. The final superposition, based on residues 16-21 in H1, 51-70 in H2 and ECL1, 132-140 in H4 and ECL2, 142-146 in ECL2, 166-182 in ECL2 and H5 and 245-283 in H6, ECL3 and H7, gave an rmsd in Cα positions of 0.66 Å for the 96 atoms and includes almost all residues involved in binding either ligand with the exception of those in H3. Using this transformation, the adenine moiety of the agonist superimposes well with the equivalent atoms of the triazolotriazene bicyclic ring of ZM241385 (rmsd 0.56 Å). Validation of the final refined models was carried out using Molprobity[43]. Omit densities for the ligands are shown in Supplementary Fig. 6. All figures in the manuscript were generated using either Pymol (DeLano Scientific) or CCPmg[31].

Binding of agonists and antagonist to A_{2A}R-GL31 expressed in CHO cells

Chinese hamster ovary (CHO) cells were maintained in culture in DMEM HAMs F12 media containing 10 % FBS. Cells were transfected with plasmids expressing either wild-type adenosine A_{2A}R or A_{2A}R-GL31 using GeneJuice according to manufacturer's instructions (EMD Biosciences). 48h after transfection, cells were harvested, centrifuged at 200 g for 5 minutes at 4° C and the pellet re-suspended in 20 mM HEPES, 10 mM EDTA buffer (pH 7.4). The membrane suspension was homogenised and centrifuged at 200 *g* for 15 minutes at

4°C. The supernatant was collected, the pellet re-suspended in 20 mM HEPES, 10 mM EDTA (pH 7.4) buffer and the solution homogenised and centrifuged as described previously[44]. The collected supernatant was centrifuged for 30 min at 40000 *g* at 4°C. Pellets were re-suspended in 20 mM Hepes, 0.1 mM EDTA to a protein concentration of 1 mg/ml and stored at −80°C .

Membranes from CHO cells transiently expressing wild-type or A_{2A}R-GL31 (10-15 μg/well) were assessed using competition [^{3}H]NECA binding in buffer containing 50 mM Tris-HCl (pH 7.4) as described previously[44]. Inhibition curves were fitted to a four-parameter logistic equation to determine IC_{50} values which were converted to K_I values using K_D values determined by saturation binding and the [^{3}H]NECA concentration of 10 nM.

G protein-coupling activity of A_{2A}R-GL31 measured in whole cells

A_{2A}R-His_6 and A_{2A}R-GL31-His_6 (amino acid residues 1-316 of human A_{2A}R) were subcloned into plasmid pcDNA5/FRT/TO using *KpnI* and *NotI* restriction sites. Flp-in T-Rex HEK293 cells were maintained at 37°C in a humidified atmosphere in Dulbecco's modified Eagle's medium without sodium pyruvate, supplemented with 4500 mg/L glucose, L-glutamine, 10% (v/v) FBS, 1 % penicillin/streptomycin mixture and 10 μg/mL blasticidin. To generate stable cell lines, the cells were transfected with a ratio of 1:9 receptor cDNA in pcDNA5/FRT/TO vector and pOG44 vector using Genejuice as per manufacturer's instructions (EMD Biosciences). After 48 h, media was replaced with fresh medium supplemented with 200 μg/mL hygromycin B to select for stably expressing clones. Colonies were combined and tested for doxycycline-induced receptor expression. To induce receptor expression clones were treated with either 1 ng/mL or 3 ng/mL doxycyline for 16 h.

Cells were seeded at a density of 25,000 per well in a poly-L-lysine coated 96-well half area plate. Cells were induced with doxycyline (3 or 1 ng/mL) for 16 h. After 16 h media was removed and replaced with fresh media containing 100 μM Ro-201724 and 2 U/mL adenosine deaminase. Cells were incubated at 37°C for 30 min prior to addition of varying concentrations of agonist (25°C, 30 min). As a control cells were also incubated for 30 min (25°C) with 10 μM forskolin. Cells were then lysed and cAMP produced detected using the CisBio cAMP kit according to manufacturer's instructions before plates were read on a PolarStar fluorescence plate reader.

References

31. Potterton L, et al. Developments in the CCP4 molecular-graphics project. Acta Crystallogr D Biol Crystallogr. 2004; 60:2288–2294. [PubMed: 15572783]
32. Weiss HM, Grisshammer R. Purification and characterization of the human adenosine A(2a) receptor functionally expressed in Escherichia coli. Eur J Biochem. 2002; 269:82–92. [PubMed: 11784301]
33. Warne T, Chirnside J, Schertler GF. Expression and purification of truncated, non-glycosylated turkey beta-adrenergic receptors for crystallization. Biochim Biophys Acta. 2003; 1610:133–140. [PubMed: 12586387]
34. Schaffner W, Weissmann C. A rapid, sensitive, and specific method for the determination of protein in dilute solution. Anal Biochem. 1973; 56:502–514. [PubMed: 4128882]
35. Gorrec F, Palmer C, Lebon G, Warne T. Pi sampling: a methodical and flexible approach to macromolecular crystallization initial screening. Acta Cryst. D. 2011 In press. [PubMed: 21543849]
36. Leslie AG. The integration of macromolecular diffraction data. Acta Crystallogr D Biol Crystallogr. 2006; 62:48–57. [PubMed: 16369093]
37. Evans P. Scaling and assessment of data quality. Acta Crystallogr D Biol Crystallogr. 2006; 62:72–82. [PubMed: 16369096]

38. McCoy AJ, et al. Phaser crystallographic software. J Appl Crystallogr. 2007; 40:658–674. [PubMed: 19461840]
39. Murshudov GN, Vagin AA, Dodson EJ. Refinement of macromolecular structures by the maximum-likelihood method. Acta Crystallogr D Biol Crystallogr. 1997; 53:240–255. [PubMed: 15299926]
40. Emsley P, Lohkamp B, Scott WG, Cowtan K. Features and development of Coot. Acta Crystallogr D Biol Crystallogr. 66:486–501. [PubMed: 20383002]
41. McDonald IK, Thornton JM. Satisfying hydrogen bonding potential in proteins. J Mol Biol. 1994; 238:777–793. [PubMed: 8182748]
42. Jones TA, Zou JY, Cowan SW, Kjeldgaard M. Improved Methods for Building Protein Models in Electron-Density Maps and the Location of Errors in These Models. Acta Crystallogr A. 1991; 47:110–119. [PubMed: 2025413]
43. Davis IW, et al. MolProbity: all-atom contacts and structure validation for proteins and nucleic acids. Nucleic Acids Res. 2007; 35:W375–383. [PubMed: 17452350]
44. Robertson N, et al. The properties of thermostabilised G protein-coupled receptors (StaRs) and their use in drug discovery. Neuropharmacology. 60:36–44. [PubMed: 20624408]

References

1. Fredholm BB, et al. International Union of Basic and Clinical Pharmacology. LXXXI. Nomenclature and Classification of Adenosine Receptors--An Update. Pharmacol Rev. 63:1–34. [PubMed: 21303899]
2. Evans BA, et al. Ligand-directed signalling at beta-adrenoceptors. Br J Pharmacol. 2010; 159:1022–1038. [PubMed: 20132209]
3. Hofmann KP, et al. A G protein-coupled receptor at work: the rhodopsin model. Trends Biochem Sci. 2009; 34:540–552. [PubMed: 19836958]
4. Rosenbaum DM, Rasmussen SG, Kobilka BK. The structure and function of G-protein-coupled receptors. Nature. 2009; 459:356–363. [PubMed: 19458711]
5. Rasmussen SG, et al. Structure of a nanobody-stabilized active state of the beta(2) adrenoceptor. Nature. 2011; 469:175–180. [PubMed: 21228869]
6. Rosenbaum DM, et al. Structure and function of an irreversible agonist-beta(2) adrenoceptor complex. Nature. 2011; 469:236–240. [PubMed: 21228876]
7. Warne T, et al. The structural basis for agonist and partial agonist action on a beta(1)-adrenergic receptor. Nature. 2011; 469:241–244. [PubMed: 21228877]
8. Jaakola VP, et al. The 2.6 angstrom crystal structure of a human A2A adenosine receptor bound to an antagonist. Science. 2008; 322:1211–1217. [PubMed: 18832607]
9. Ballesteros JA, Weinstein H. Integrated methods for the construction of three dimensional models and computational probing of structure function relations in G protein-coupled receptors. Methods Neurosci. 1995; 25:366–428.
10. Kobilka BK, Deupi X. Conformational complexity of G-protein-coupled receptors. Trends Pharmacol Sci. 2007; 28:397–406. [PubMed: 17629961]
11. Yao XJ, et al. The effect of ligand efficacy on the formation and stability of a GPCR-G protein complex. Proc Natl Acad Sci U S A. 2009; 106:9501–9506. [PubMed: 19470481]
12. Vauquelin G, Van Liefde I. G protein-coupled receptors: a count of 1001 conformations. Fundam Clin Pharmacol. 2005; 19:45–56. [PubMed: 15660959]
13. Palczewski K, et al. Crystal structure of rhodopsin: A G protein-coupled receptor. Science. 2000; 289:739–745. [PubMed: 10926528]
14. Li J, et al. Structure of bovine rhodopsin in a trigonal crystal form. J Mol Biol. 2004; 343:1409–1438. [PubMed: 15491621]
15. Park JH, et al. Crystal structure of the ligand-free G-protein-coupled receptor opsin. Nature. 2008; 454:183–187. [PubMed: 18563085]
16. Scheerer P, et al. Crystal structure of opsin in its G-protein-interacting conformation. Nature. 2008; 455:497–502. [PubMed: 18818650]

17. Cherezov V, et al. High-resolution crystal structure of an engineered human beta2-adrenergic G protein-coupled receptor. Science. 2007; 318:1258–1265. [PubMed: 17962520]
18. Rasmussen SG, et al. Crystal structure of the human beta2 adrenergic G-protein-coupled receptor. Nature. 2007; 450:383–387. [PubMed: 17952055]
19. Warne T, et al. Structure of a beta1-adrenergic G-protein-coupled receptor. Nature. 2008; 454:486–491. [PubMed: 18594507]
20. Wu B, et al. Structures of the CXCR4 chemokine GPCR with small-molecule and cyclic peptide antagonists. Science. 2010; 330:1066–1071. [PubMed: 20929726]
21. Chien EY, et al. Structure of the human dopamine D3 receptor in complex with a D2/D3 selective antagonist. Science. 2010; 330:1091–1095. [PubMed: 21097933]
22. Oldham WM, Hamm HE. Heterotrimeric G protein activation by G-protein-coupled receptors. Nat Rev Mol Cell Biol. 2008; 9:60–71. [PubMed: 18043707]
23. Murphree LJ, et al. Human A(2A) adenosine receptors: high-affinity agonist binding to receptor-G protein complexes containing Gbeta(4). Mol Pharmacol. 2002; 61:455–462. [PubMed: 11809871]
24. Serrano-Vega MJ, Magnani F, Shibata Y, Tate CG. Conformational thermostabilization of the beta1-adrenergic receptor in a detergent-resistant form. Proc Natl Acad Sci U S A. 2008; 105:877–882. [PubMed: 18192400]
25. Magnani F, Shibata Y, Serrano-Vega MJ, Tate CG. Co-evolving stability and conformational homogeneity of the human adenosine A2a receptor. Proc Natl Acad Sci U S A. 2008; 105:10744–10749. [PubMed: 18664584]
26. Shibata Y, et al. Thermostabilization of the neurotensin receptor NTS1. J Mol Biol. 2009; 390:262–277. [PubMed: 19422831]
27. Kim SK, et al. Modeling the adenosine receptors: comparison of the binding domains of A2A agonists and antagonists. J Med Chem. 2003; 46:4847–4859. [PubMed: 14584936]
28. Dal Ben D, et al. Adenosine receptor modeling: what does the A2A crystal structure tell us? Curr Top Med Chem. 10:993–1018. [PubMed: 20370656]
29. Wacker D, et al. Conserved binding mode of human beta2 adrenergic receptor inverse agonists and antagonist revealed by X-ray crystallography. J Am Chem Soc. 2010; 132:11443–11445. [PubMed: 20669948]
30. Xu F, et al. Structure of an Agonist-Bound Human A2A Adenosine Receptor. Science. 2011 DOI: 10.1126/science.1202793. [PubMed: 21393508]

Europe PMC Funders Author Manuscripts

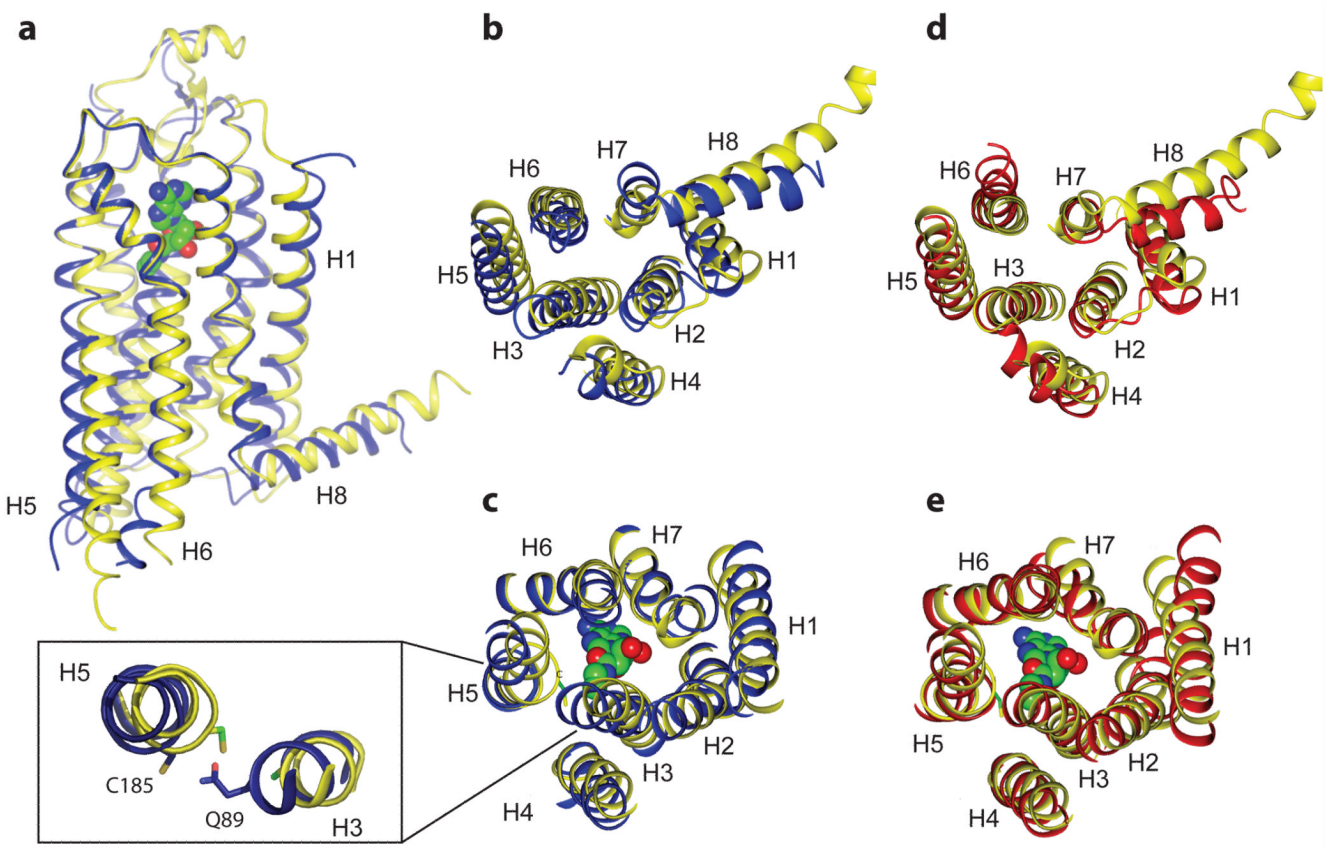

Figure 1.

Structure of the adenosine A_{2A} receptor bound to NECA compared to other GPCR structures. (a) The structure of NECA-bound $A_{2A}R$ is shown as a cartoon (yellow) aligned with the structure of A_{2A}-T4L bound to the inverse agonist ZM241385 (blue; PDB code 3EML[8]). NECA is shown as a space-filling model (C, green; N, blue; O, red). (b, c) Sections through the aligned receptors in (a) to highlight the differences in the intracellular face of the receptors (b) and in the ligand binding pocket (c), with the bulge in H5 shown as an inset. (d, e) Alignment of NECA-bound $A_{2A}R$ (yellow) with agonist-bound β_2AR-Nb80 (red; PDB code 3P0G[5]) showing the intracellular face of the receptors (d) and the ligand binding pocket (e). NECA is shown as a space-filling model in c and e. The figures were generated using CCP4mg[31]. Analogous alignments to opsin are depicted in Supplementary Fig. 7.

Europe PMC Funders Author Manuscripts

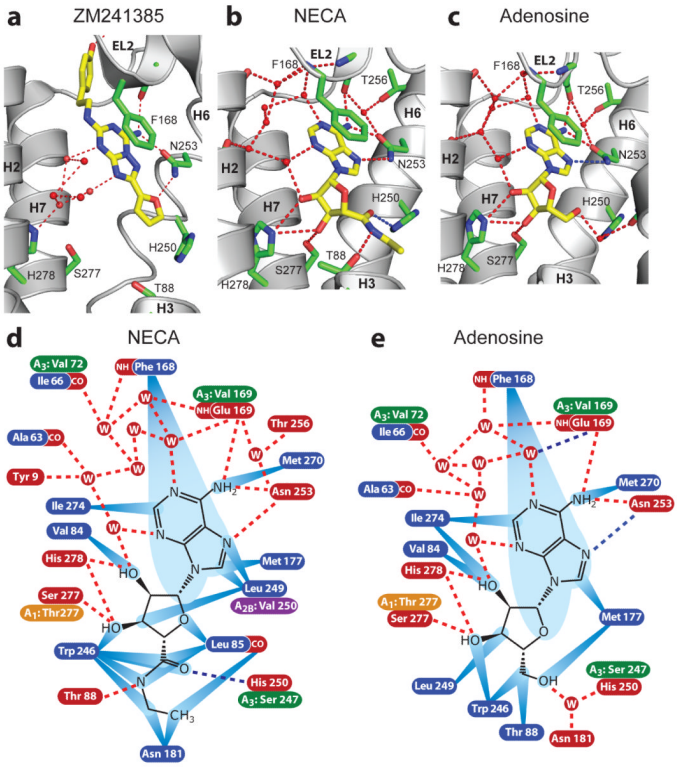

Figure 2.

Receptor-ligand interactions compared for the adenosine receptor bound to the inverse agonist ZM241385 and the agonists NECA and adenosine. Structures of the human $A_{2A}R$ in cartoon representation are shown bound to the following ligands: (a) ZM241385 (PDB code 3EML[8]); (b) NECA; (c) adenosine. (d, e) Polar and non-polar interactions involved in agonist binding to $A_{2A}R$ are shown for NECA (d) and adenosine (e). Amino acid residues within 3.9 Å of the ligands are depicted, with residues highlighted in blue making van der Waals contacts (blue rays) and residues highlighted in red making potential hydrogen bonds with favourable geometry (red dashed lines, as identified by HBPLUS, see Methods Online) or hydrogen bonds with unfavourable geometry (blue dashed lines, donor acceptor distance less than 3.6 Å). Where the amino acid residue differs between the human $A_{2A}R$ and the human A_1R, $A_{2B}R$ and A_3R, the equivalent residue is shown highlighted in orange, purple or green, respectively. Panels a-c were generated using Pymol (DeLano Scientific Ltd). Omit densities for the ligands are shown in Supplementary Fig. 6 and densities for water molecules in Supplementary Fig. 8.

Europe PMC Funders Author Manuscripts

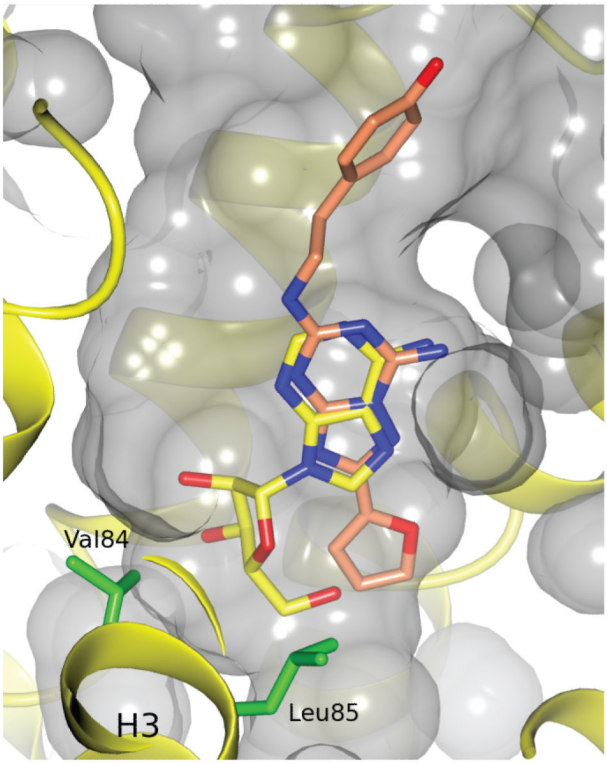

Figure 3.

Positions of adenosine and ZM241385 in the adenosine A_{2A} receptor ligand binding pocket. The structures of adenosine-bound A_{2A}R-GL31 and ZM241385-bound A_{2A}-T4L were aligned using only atoms from the protein to allow the ligand positions to be compared, with adenosine in yellow and ZM241385 in pink (N, blue; O, red). The ligands are shown in the context of the binding pocket of A_{2A}R-GL31, with transmembrane helices of A_{2A}R-GL31 shown in yellow and the surfaces of the receptor, including the cavity of the ligand binding pocket, shown in grey. The side chains of Val84 and Leu85 that interact with the ribose moiety of the agonist are shown in green.

Europe PMC Funders Author Manuscripts

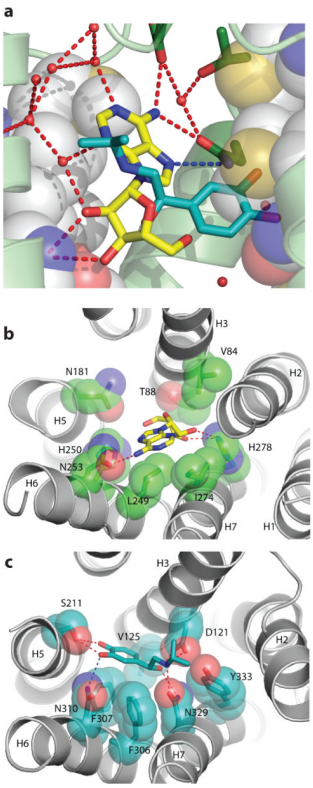

Figure 4.

Comparison of the positions of agonists in the binding pockets of the adenosine A_{2A} receptor and a β-adrenoceptor. (a) The structures of $A_{2A}R$ bound to adenosine and β_1AR bound to isoprenaline (PDB code 2Y03)[7] were aligned by superimposing equivalent atoms in the protein structure and the positions of both ligands shown as stick models with the carbon atoms in blue-green (isoprenaline) or yellow (adenosine) nitrogen in blue and oxygen in red. The $A_{2A}R$ structure is shown, with H5 and H7 as space-filling models (C, grey; N, blue; O, red) and the remainder of the structure as a cartoon (pale green). Some water molecules are shown as red spheres, hydrogen bonds as red dashed lines and the polar contacts as blue dashed lines. The orientation of the figure is identical to that shown in Fig. 2. (b) Structure of $A_{2A}R$ bound to adenosine viewed from the extracellular surface. (c) Structure of β_1AR bound to isoprenaline (PDB code 2Y03)[7] viewed from the extracellular surface. In panels b and c, equivalent side chains in the respective structures that make contacts to both isoprenaline and adenosine in their respective receptors are shown as space-filling models and they have the following Ballesteros-Weinstein numbers (amino acid side chains are shown in parentheses for the $A_{2A}R$ and β_1AR, respectively): 3.32 (V84, D121); 3.36 (T88, V125); 5.42 (N181*, S211); 6.51 (L249, F306); 6.55 (N253, N310); 6.52 (H250*, F307); 7.39 (I274, N329); 7.43 (H278, Y333). Some residues (*) only make indirect contacts to the agonists via a water molecule.